Retardation and repair of fatigue cracks in a microcapsule toughened epoxy composite—Part I: Manual infiltration

E.N. Brown[1,*], S.R. White[2], N.R. Sottos[1]

[1] Department of Theoretical and Applied Mechanics and the Beckman Institute for Advanced Science and Technology, University of Illinois at Urbana-Champaign, Urbana, IL 61801, USA

[2] Department of Aerospace Engineering and the Beckman Institute for Advanced Science and Technology, University of Illinois at Urbana-Champaign, Urbana, IL 61801, USA

[*] Corresponding Author. Present address: Materials Science and Technology Division, Los Alamos National Laboratory, MS-E544, Los Alamos, NM 87545, USA. Tel: 1(505)667-0799, Fax: 1(505)667-2185.

E-mail address: en_brown@lanl.gov (E.N. Brown).

Abstract

As a first step towards a new crack healing methodology for cyclic loading, this paper examines two promising crack-tip shielding mechanisms during fatigue of a microcapsule toughened epoxy. Artificial crack closure is achieved by injecting precatalyzed monomer into the crack plane to form a polymer wedge at the crack tip. The effect of wedge geometry is also considered, as dictated by crack loading conditions during infiltration. Crack-tip shielding by a polymer wedge formed with the crack held open under the maximum cyclic loading condition (K_{max}) yields temporary crack arrest and extends the fatigue life by more than 20 times. Hydrodynamic pressure and viscous damping as a mechanism of crack tip shielding are also investigated by injecting mineral oil into the crack plane. Viscous fluid flow leads to retardation of crack growth independent of initial loading conditions. The success of these mechanisms for retarding fatigue crack growth demonstrates the potential for *in situ* self-healing of fatigue damage.

Keywords: A. smart materials, A. polymer-matrix composites, B. fatigue, C. failure criterion, self-healing

Submitted for publication in *Composites Science and Technology* (2005)

1. Introduction

Thermosetting polymers are used in a wide variety of applications ranging from structural composites to microelectronics. Due to low strain-to-failure, these polymers are highly susceptible to damage in the form of cracks. In structural composites these cracks can lead to fiber/matrix debonding and inter-ply delamination, ultimately resulting in component failure. Susceptibility to cyclic loading is particularly problematic because a crack will grow, however slowly, above a threshold range of stress intensities ΔK_{th} that is significantly lower than the critical stress intensity K_{IC}. Prevention of fatigue failure currently depends on accurate life prediction and implementation of inspection procedures.

Polymer fatigue has been studied extensively in both homogeneous and composite structures (*e.g.*, [1–15]). In most polymers, fatigue crack growth rates (da/dN) are accurately described by the Paris power law [16],

$$\frac{\mathrm{d}a}{\mathrm{d}N} = C_0 \Delta K_{\mathrm{I}}^{n}, \tag{1}$$

where C_0 and n are material constants and ΔK_{I} is the applied range of stress intensity. Typical Paris power law crack growth behavior is shown schematically by the solid curve in Fig. 1. Despite this understanding of cyclic crack growth, fatigue failure remains a major cause of component failure.

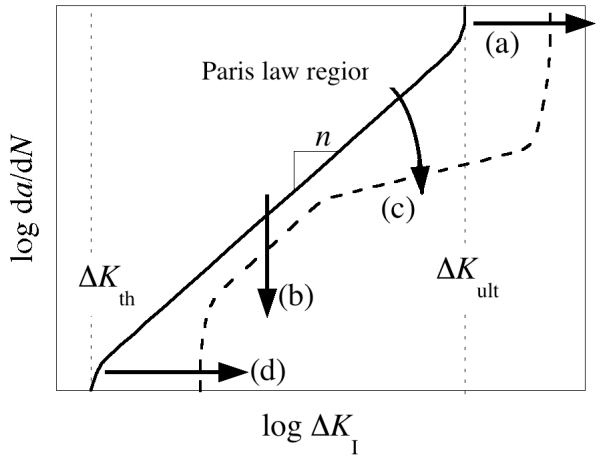

Fig. 1. Representative relationship between fatigue crack growth rate (da/dN) and the applied stress intensity range (ΔK_{I}) in the Paris power law region. Improved fatigue behavior can be obtained by: (a) increasing the range of stress intensity before crack growth instability ΔK_{ult}, (b) reducing the crack growth rate da/dN for a given ΔK_{I}, (c) reducing the crack growth rate sensitivity to ΔK_{I}, *i.e.* reduce n, or (d) increasing the threshold ΔK_{th} at which crack growth arrests.

Strategies for improving fatigue life are shown schematically in Fig. 1 and include: (a) increasing the range of stress intensity before crack growth instability ΔK_{ult}, (b) decreasing the crack growth rate da/dN for a given ΔK_{I}, (c) decreasing the crack

growth rate sensitivity to ΔK_I, *i.e.* reduce n, and (d) increasing the threshold ΔK_{th} at which crack growth arrests. In the case of brittle thermosetting polymers, incorporation of a rubbery second phase [8–10], solid particles [11–13] or microcapsules [14,15] significantly improves fatigue performance by increasing the fracture toughness (Fig. 1a) and decreasing the Paris power law exponent (Fig. 1c). Of relevance for the current work, the presence of liquid-filled microcapsules increases the fracture toughness of epoxy by up to 127% [17]. The addition of microcapsules also significantly decreases the Paris power law exponent above a transition value of the stress intensity factor ΔK_T [14]. In this regime, the Paris power law exponent decreases from approximately 10 for neat epoxy to 4.5 for concentrations above 10 wt% microcapsules.

In contrast to steady-state crack growth described by the Paris power law, many fatigue response mechanisms evolve over the course of loading, causing the fatigue crack growth rate to accelerate or decelerate under constant ΔK_I. Crack-tip shielding mechanisms such as crack closure can significantly retard fatigue crack growth. Initial work on crack closure by Elber [18,19] is based on the development of a local plastic zone that shields the crack tip such that the crack tip stress state cannot unload beyond $K_{closure}$ (Fig. 2b). This shielding mechanism leads to a local driving force for fatigue ΔK_{eff} that is less than the applied ΔK_I, and effectively reduces the crack growth rate.

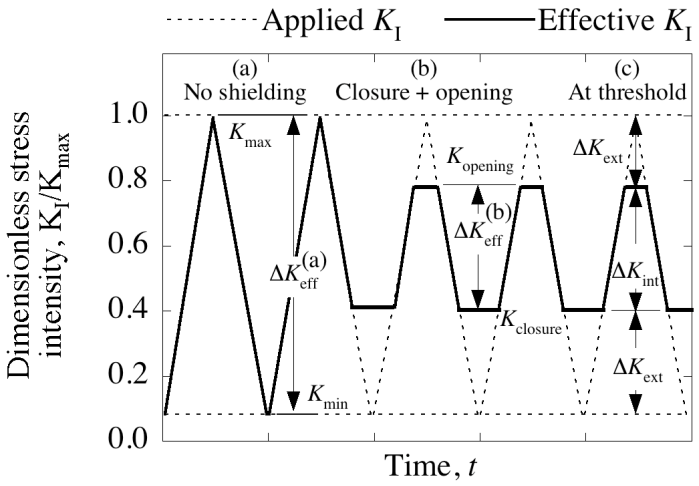

Fig. 2. Schematic of cyclic loading profile with crack-tip shielding nomenclature for three conditions: (a) no shielding ($\Delta K_{eff} = \Delta K_I$), (b) shielding from crack closure preventing unloading to K_{min}, and (c) combined shielding from K_{max} and K_{min} (adapted from Sharp, Clayton, and Clark [23]).

More recently, artificial crack closure induced by infiltration of a polymer was reported to reduce constant ΔK_I fatigue crack growth and increase the fatigue threshold in metals [20]. Cyclic loading was halted after the fatigue crack had grown significantly and an uncured polymer resin was injected into the crack plane. Once the resin cured, constant ΔK_I cyclic loading was resumed. The presence of the polymer wedge prevented full unloading at the crack tip, increased the effective minimum value of the cyclic stress intensity (from K_{min} to $K_{closure}$) and reduced the local driving force for fatigue ΔK_{eff}, even

though the applied ΔK_I dictated by far-field loading was unchanged. Fatigue life-extensions from 100% [20,21] to 1000% [22,23] were observed with polymer infiltration. The cyclic loading profiles of the applied ΔK_I and ΔK_{eff} arising from the crack closure mechanism are illustrated schematically in Fig. 2a,b (adapted from [23]). Although Sharp et al. [23] proposed a further reduction of ΔK_{eff} could be achieved by reducing the crack tip opening and thereby decreasing the effective maximum value of the cyclic stress intensity from K_{max} to $K_{opening}$ (Fig. 2c), this mechanism led to negligible increases in fatigue life.

Hydrodynamic pressure crack-tip shielding due to viscous flow within a fatigue crack has also been reported to decrease the effective range of mode-I stress intensity and reduce fatigue crack growth rate [24,25]. These investigations were restricted to metals and performed with the specimens immersed in the fluid of interest. The forces required to squeeze a viscous fluid out of the crack during unloading and draw fluid into the crack during loading provided effective crack-tip shielding. Crack growth rates measured in oils were lower than in air. Greater reductions in crack growth rate occurred for higher viscosity oils [26–28], until an upper limit was reached and the fluid could no longer penetrate to the crack tip [29,30]. For metals, crack-tip shielding from hydrodynamic pressure provided nearly 50% reduction in crack growth rate [29,31].

In this work, we present a new methodology for retardation and repair of fatigue cracks based on the self-healing concept developed by White et al. [32]. In Part I we investigate two crack-tip shielding mechanisms during fatigue of a microcapsule toughened epoxy. Artificial crack closure is achieved by injecting precatalyzed monomer into the crack plane to form a polymer wedge at the crack tip. Hydrodynamic pressure and viscous damping at the crack tip are investigated by injecting mineral oil into the crack plane. Building on the success of these mechanisms for retarding fatigue crack growth, Part II [33] reports on *in situ* self-healing of fatigue damage.

2. Fatigue test method

2.1. Materials and sample preparation

Urea-formaldehyde microcapsules containing dicyclopentadiene (DCPD) monomer were manufactured with average diameter of 180 μm using the emulsion *in situ* polymerization microencapsulation method outlined by Brown et al. [34]. Shell wall thickness was 190 ± 30 nm for all batches. Tapered double-cantilever beam specimens were cast from EPON® 828 epoxy resin (DGEBA) and 12 pph Ancamine® DETA (diethylenetriamine) curing agent with 20 wt% of microcapsules mixed into the resin. For the work presented in this paper the effect of *in situ* self-healing was excluded by omitting the catalyst phase in the resin formulation. The epoxy mixture was degassed, poured into a closed silicone rubber mold and cured for 24 hours at room temperature, followed by 24 hours at 30° C. Relevant physical and material properties are listed in Table 1.

Table 1
Properties of the constituent materials [14]

Property	Epoxy	Urea-formaldehyde microcapsules	Epoxy with 20 wt% microcapsules
K_{IC} (MPa $m^{1/2}$)	0.55±0.04	—	1.0±0.2
Young's modulus (GPa)	3.4±0.1	—	2.7±0.1
Paris power law exponent, n	9.7	—	4.3
Paris power law constant, C_0	8.2×10^{-2}	—	3.8×10^{-4}
Density (kg/m^3)	1160	~1000	~1120
Diameter (μm)	—	180±40	—
Wall thickness (nm)	—	190±30	—

2.2. *Mechanical testing*

The fatigue-crack propagation behavior of microcapsule toughened epoxy was investigated using the tapered double-cantilever beam (TDCB) specimen geometry, shown in Fig. 3. The fatigue experiment and specimen geometry are outlined by Brown et al. in [14] and [35], respectively. Side grooves are included to ensure controlled crack growth along the centerline of the brittle specimen. The TDCB geometry, developed by Mostovoy et al. [36], provides a crack-length-independent relationship between applied stress intensity factor K_I and load P,

$$K_I = \alpha P, \tag{2}$$

which only requires knowledge of the coefficient α = 11.2x10^3 $m^{-3/2}$ [34]. A constant range of mode-I stress intensity factor ΔK_I was achieved by applying a constant range of applied load ΔP, independent of crack length.

Fatigue crack propagation studies were performed using an Instron DynoMight 8841 low-load frame with 250 N load cell. Samples were precracked with a razor blade while ensuring the precrack tip was centered in the groove and then pin loaded. A

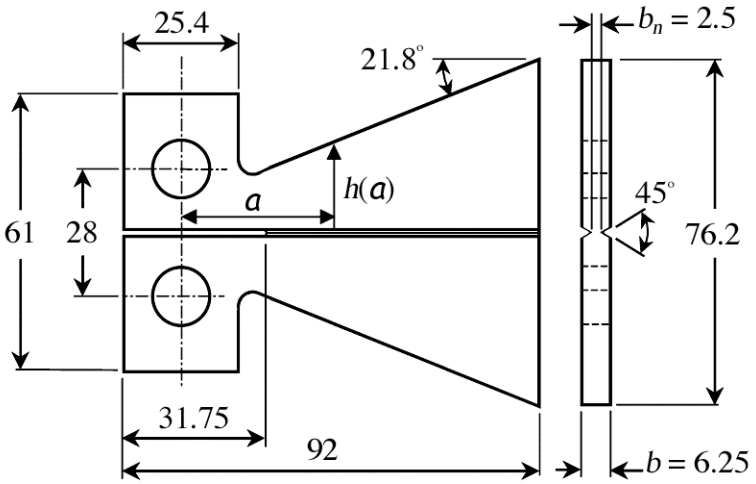

Fig. 3. Tapered-double-cantilever-beam geometry [35]. All dimensions in mm.

triangular frequency of 5 Hz was applied with a load ratio ($R = K_{min}/K_{max}$) of 0.1. Fatigue cracks were grown under mode-I stress intensity factor range $\Delta K_I = 0.473$ MPa $m^{1/2}$. Crack lengths were measured optically and by specimen compliance [14]. First, the optically measured crack-tip position and specimen compliance were plotted against number of cycles. A linear relationship between crack length and specimen compliance was then used to calculate the crack-tip position at all times during the experiment.

The constant ΔK nature of the fatigue test yields a constant crack-growth rate over the majority of the length of the specimen. The degree of observed crack acceleration fluctuates with loading conditions and sample material. In the absence of secondary shielding mechanisms, the rate is defined by the Paris power law dependence on the applied range of mode-I stress intensity factor ΔK_I [14]. Any deviation during a given test (*e.g.* crack growth retardation or arrest) is therefore an isolated effect of either viscous flow or artificial crack closure. To account for the complexity associated with changing fatigue crack growth rates under cyclic loading conditions, fatigue-healing efficiency is defined by fatigue life-extension,

$$\lambda = \frac{N_{healed} - N_{control}}{N_{control}}, \tag{3}$$

where N_{healed} is the total number of cycles to failure for a self-healing sample and $N_{control}$ is the total number of cycles to failure for a similar sample without healing.

3. Results

Healing under fatigue loading was first investigated by manual injection of precatalyzed healing agent in the crack plane (DCPD mixed with 2 g L^{-1} of Grubbs' first generation Ru catalyst). Healing agent was injected into the crack plane under three loading conditions: zero-load, constant K_{max}, and continuous cyclic loading. For a control experiment, a fatigue crack was grown in a sample without injection until failure occurred ($N_{control} = 1.71 \times 10^5$ cycles). Infiltration of a viscous fluid (with no polymerization) was also explored for an additional comparison case.

For the zero-load case, a crack was grown for several mm at which point fatigue loading was interrupted, precatalyzed healing agent was injected into the crack plane, and all external loads were removed from the sample. Fatigue loading was reestablished after a 10 h healing (cure) period at room temperature. The crack-tip position is plotted against number of cycles for this case in Fig. 4. Following healing, the crack retreated to the approximate location of the sample prenotch. Upon the resumption of cyclic loading, an interfacial crack rapidly initiated between the polyDCPD and epoxy and propagated to the crack-tip position prior to healing. Crack growth in the neat epoxy commenced at its prehealed rate until sample failure. The fatigue-healing efficiency λ defined by Eq. (3) and calculated using the data from the control sample was less than 1%.

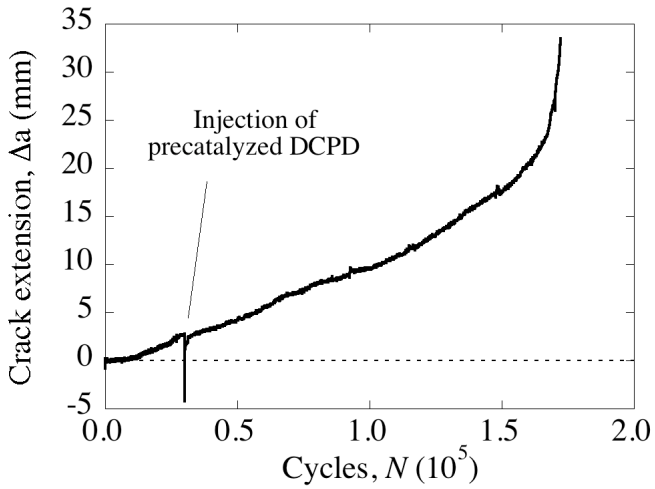

Fig. 4. Crack length *vs*. fatigue cycles of manual injection sample healed under zero-load and tested to failure, $\lambda < 1\%$. $\Delta K_I = 0.473$ MPa m$^{1/2}$, $K_{max} = 0.525$ MPa m$^{1/2}$, $K_{min} = 0.053$ MPa m$^{1/2}$, $R = 0.1$, $f = 5$ Hz, and $a_0 = 24.3$ mm.

For the second loading case, a crack was grown for several mm, fatigue loading was interrupted, the sample was held at constant K_{max}, and precatalyzed healing agent was injected into the crack plane. Fatigue loading was reestablished after a 10 h healing period at room temperature. Crack-tip position is plotted against number of cycles for this case in Fig. 5. Crack growth through the polyDCPD region exhibited three regimes of relatively stable crack-tip position. After significant life extension, crack growth in the toughened epoxy resumed at its prehealed growth rate. Sample failure of the healed specimen occurred after $N_{healed} = 3.68 \times 10^6$ total applied cycles. For this case, the fatigue-healing efficiency λ defined by Eq. (3) was 2000%.

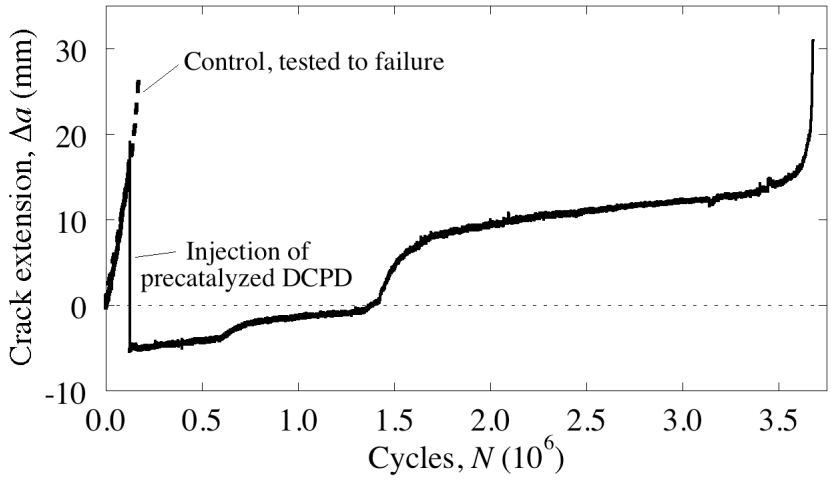

Fig. 5. Crack length *vs*. fatigue cycles of manual injection sample healed under K_{max} and control sample tested to failure, $\lambda = 2052\%$. $\Delta K_I = 0.473$ MPa m$^{1/2}$, $K_{max} = 0.525$ MPa m$^{1/2}$, $K_{min} = 0.053$ MPa m$^{1/2}$, $R = 0.1$, $f = 5$ Hz, and $a_0 = 26.1$ mm.

The load–displacement response changes significantly over the course of the sample fatigue life, shown in Fig. 6. In the early cycles, prior to injection of DCPD, the load–displacement relationship is linear with increasing compliance as the crack propagates. Following healing agent injection and polymerization at K_{max}, the load–displacement relationship remains linear with a reduced compliance. After numerous cycles without crack advance, the load–displacement curve becomes bimodal. The portion of the load–displacement curve above the knee becomes increasingly compliant as the crack length increases. Simultaneously, the knee occurs at decreasing load levels. Crack growth approaches the prehealed rate when the load–displacement curves return to a linear regime.

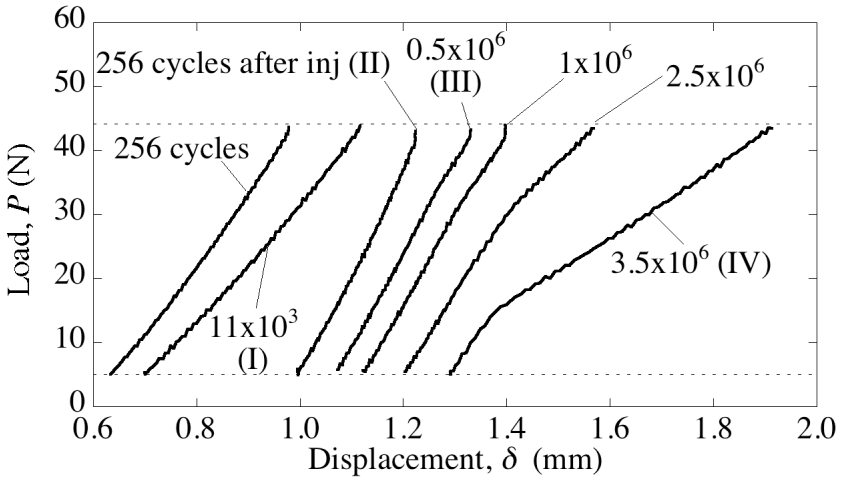

Fig. 6. Load–displacement curves for select cycles corresponding with Fig. 5.

For the continuous cyclic loading case, a crack was grown for several mm at which point precatalyzed healing agent was injected into the crack plane. The DCPD flowed backward and forward in the fracture plane corresponding to the closing and opening of the crack. The extent of flow decreased with time as the DCPD polymerized in the crack plane. Immediately following injection, the sample compliance decreased slightly and the crack arrested for the first 1.5 h following injection (2.7×10^4 cycles). Following gelation, the increased stiffness of the rubbery polymer appeared as a regression of the crack tip. Once the polyDCPD reached the glassy regime—characterized by the degree of cure for the glass transition temperature to exceed the ambient temperature [37]—the crack tip stabilized until debonding initiated. The fatigue life-extension λ associated with the temporary crack growth retardation shown in Fig. 7 was 56%.

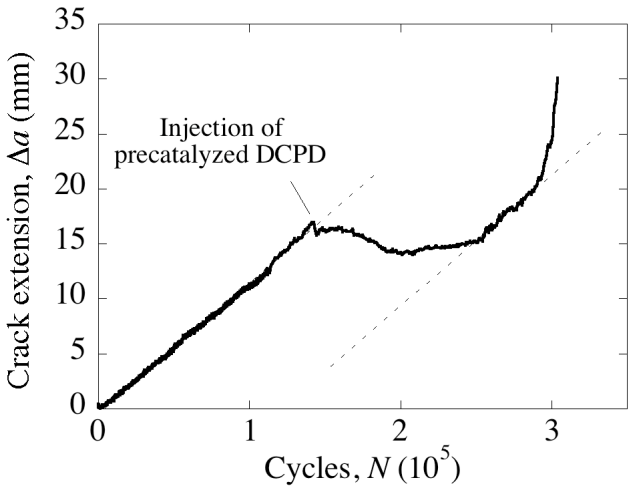

Fig. 7. Crack length *vs*. fatigue cycles of manual injection sample healed under continuous cyclic loading and tested to failure, $\lambda = 55.9\%$. $\Delta K_I = 0.473$ MPa m$^{1/2}$, $K_{max} = 0.525$ MPa m$^{1/2}$, $K_{min} = 0.053$ MPa m$^{1/2}$, $R = 0.1$, $f = 5$ Hz, and $a_0 = 22.9$ mm.

For comparative purposes, infiltration of a non-healing viscous fluid was also investigated. A crack was grown for several mm in a microcapsule-toughened epoxy sample and mineral oil (Fisher Scientific, New Jersey) was injected into the crack plane. Injection of mineral oil—an inert hydrocarbon oligomeric compound with a viscosity (30 cP at 40°C) approximately 40 times higher than DCPD—dramatically reduced the crack growth rate (Fig. 8). Unlike the case of a submerged sample, where crack growth rates are reported to be steady [25], the retarded crack growth exhibited significant variability. Notably, crack growth retardation lagged the injection event, potentially due to the time required for the oil to be drawn into the crack tip. After a period of arrest, the

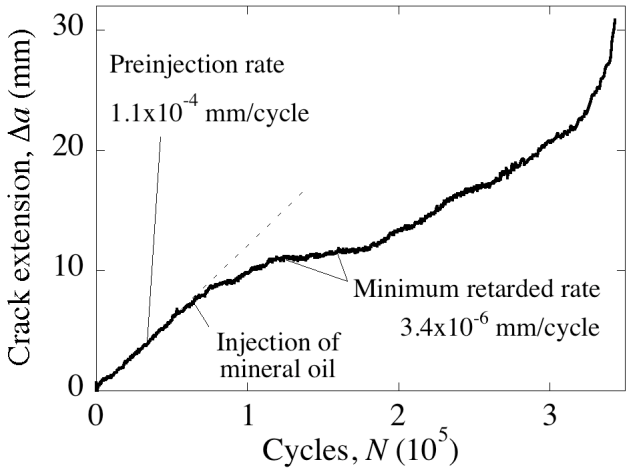

Fig. 8. Crack length *vs*. number of cycles for manual injection of mineral oil $\lambda = 101\%$. Hydrodynamic pressure from the viscous fluid dramatically reduces the crack growth rate and leads to significant life extension. $\Delta K_I = 0.473$ MPa m$^{1/2}$, $K_{max} = 0.525$ MPa m$^{1/2}$, $K_{min} = 0.053$ MPa m$^{1/2}$, $R = 0.1$, $f = 5$ Hz, and $a_0 = 21.4$ mm.

crack growth rate increased (although never resuming the preinjection rate) in combination with an observed loss of oil from the crack plane.

4. Discussion

Manual injection of precatalyzed monomer healing agent extends the fatigue life of microcapsule toughened epoxy through a combination of crack-tip shielding mechanisms. In samples injected with precatalyzed DCPD and healed at K_{max}, crack closure due to the formation of a polyDCPD wedge at the crack tip provides the dominant shielding mechanism for fatigue crack retardation (Fig. 5). Conversely, the wedge polymerized at zero-load does not result in any crack-tip shielding through artificial crack closure (Fig. 4). As described previously for metals [21], a polymer wedge formed at or above K_{max} provides maximum shielding efficiency and approaches a stress free crack tip. Shin, Huang and Li [23] have also reported that injection must occur at K_{max} or larger to achieve any significant fatigue crack retardation.

The success of crack closure is strongly dependent on how efficiently the crack tip is shielded from the applied cyclic loads. The progression of the load–displacement curves in Fig. 6 is representative of crack closure and correlates well with the temporary crack arrest events observed in Fig. 5 following injection at K_{max}. The stages of the crack closure mechanism are summarized schematically in Fig. 9. In the early cycles prior to injection of DCPD (Fig. 9a,b), the corresponding load–displacement curve in Fig. 6 (curve I) is linear with increasing compliance as the crack propagates. Following healing agent injection and cure (Fig. 9c,d), the load–displacement curve in Fig. 6 (curve II) remains linear with a reduced compliance due to the shorter, healed crack length. After numerous cycles without crack advance, the load–displacement curve becomes bimodal (Fig. 6, curve III), representative of the crack closure mechanism proposed by Elber [18]. The portion of the load–displacement curve above the knee, which represents the open crack condition and the portion of the cyclic load experienced by the crack tip, become increasingly compliant indicating progressive debonding of the healed DCPD interface as shown Fig. 9e. The portion of the load–displacement curve below the knee, which represents the closed crack condition (Fig. 9f), retains a compliance corresponding to the healed crack geometry. Simultaneously, the knee occurs at decreasing loads, indicating an increase in the effective cyclic stress intensity at the crack tip. As the crack grows past the DCPD wedge (Fig. 9g,h), the crack growth rate increases with increasing ΔK_{eff} approaching the prehealed rate and proceeds in this fashion until sample failure.

Hydrodynamic pressure at the crack tip associated with viscous healing agent in the crack plane also provides a shielding mechanism in microcapsule toughened epoxy. Injection experiments with both catalyzed healing agent (Fig. 7) and mineral oil (Fig. 8) demonstrate reduced crack growth rates. The effectiveness of DCPD at providing shielding by hydrodynamic pressure is dependent on the degree of cure (α). Low viscosity DCPD monomer ($\alpha = 0$) has a low resistance to flow, providing nominal crack-tip shielding. As the degree of cure and viscosity increase, significant crack growth retardation is obtained. Further polymerization leads to crack regression as the shielding mechanism transitions from hydrodynamic pressure to crack closure.

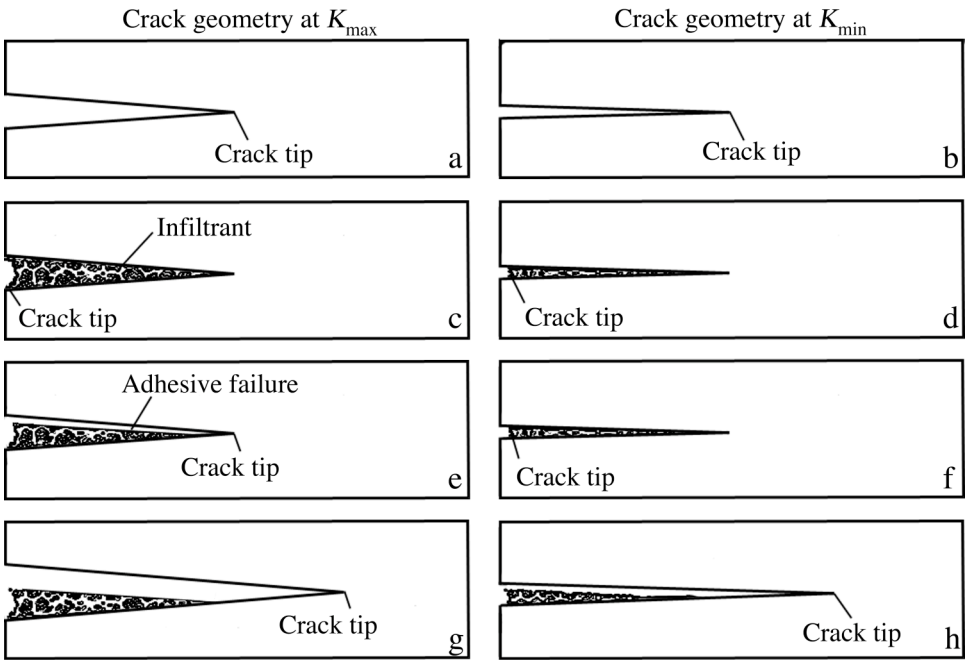

Fig. 9. Schematic summary of crack closure mechanism and the apparent crack-tip positions for K_{max} and K_{min} loading conditions: (a) original crack at maximum crack opening, and (b) at minimum opening (Fig. 6, curve I), (c,d) crack closure immediately after crack is filled with infiltrant (curve II), (e,f) following crack growth through the infiltrant, which is accompanied by onset of a bimodal compliance curve (curve III), and (g,h) after crack growth past the infiltrant, which is accompanied by diminished crack-tip shielding from artificial crack closure (curve IV).

The shielding effect of hydrodynamic pressure has been modeled analytically [29,30] and numerically [38] for fatigue crack growth in metals. As shown schematically in Fig. 10, the effective loading at a viscous fluid-filled crack tip lags behind and has a significantly different shape than the applied cyclic stress intensity profile. The models predict a reduction of crack growth rates for increased fluid viscosity, lower stress ratios R, lower applied ranges of stress intensity ΔK_I, larger crack thickness b, and higher cyclic frequencies f. Because fatigue crack growth in metals is less sensitive to changes in ΔK_I (Paris power law exponent $n \sim 3$), partial shielding yields only a modest reduction in crack growth rate, with greater potential for brittle polymers ($n = 4.5$–10), as demonstrated in the current work.

5. Conclusions

Experiments were performed to elucidate mechanisms of fatigue crack growth retardation and arrest in microcapsule-toughened epoxy. A protocol based on fatigue life-extension was established for measuring crack healing efficiency under cyclic loading. Fatigue life-extension was achieved by a combination of crack-tip shielding mechanisms. Viscous flow of the healing agent in the crack plane retarded the crack growth process. Polymerization of the healing agent led to a short term adhesive effect and a long term crack closure effect, which prevented full unloading of the crack tip.

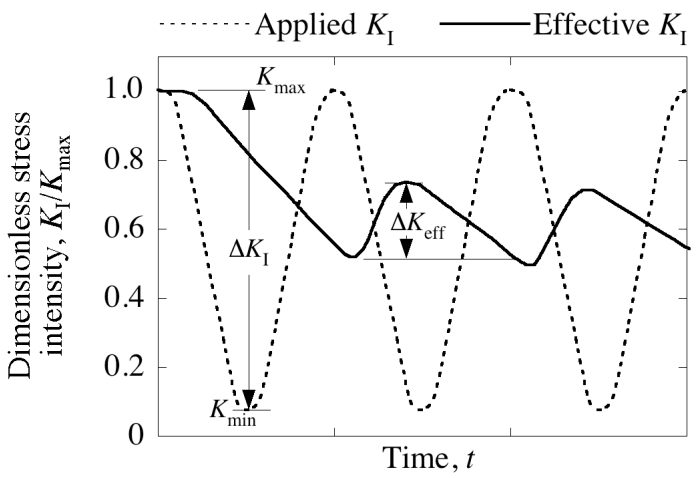

Fig. 10. Reduced effective crack-tip stress intensity due to hydrodynamic pressure from a viscous fluid-filled crack (adapted from Yi, Cox, and Dauskardt [38]). Note: The effective and applied K_I are both equal to K_{max} at $t = 0$ until viscous damping produces the steady-state condition in the second cycle.

Significant fatigue-crack retardation was achieved by artificial crack closure induced by a polymerized healing agent (DCPD) wedge at the crack tip that prevented full crack-tip unloading. Moreover, successful crack closure was independent of the adhesive strength of the interface. Crack closure from the polymer wedge continued to retard crack growth long after the crack started to propagate through the healed region.

The mechanisms for retardation and repair associated with manual injection represent the first steps towards a new crack healing methodology. Further development of this methodology is presented in Part II of this paper [33] where retardation and repair of fatigue cracks is achieved through *in situ* self-healing.

Acknowledgments

The authors gratefully acknowledge support from the AFOSR Aerospace and Materials Science Directorate Mechanics and Materials Program (Award No. F49620-02-1-0080), the National Science Foundation (NSF CMS0218863), and Motorola Labs, Motorola Advanced Technology Center, Schaumburg Ill. The authors would also like to thank Profs. J.S. Moore and P.H. Geubelle of the University of Illinois and Dr. A. Skipor of Motorola Labs for technical support and helpful discussions.

References

[1] Skibo MD, Hertzberg RW, Manson JA, Kim SL. On the generality of discontinuous fatigue growth in glassy polymers. J Mater Sci 1977;12(3):531–542.

[2] Radon JC. Fatigue growth in polymers. Int J Fract 1980;16(6):533–551.

[3] Sauer JA, Richardson GC. Fatigue of polymers. Int J Fract 1980:16(6):499–532.
[4] Szabo JS, Gryshchuk O, Karger-Kocsis J. Fatigue crack propagation behavior of interpenetrating vinylester/epoxy resins. J Mater Sci Letters 2003;22(16):1141–1145.
[5] Kawaguchi T, Pearson RA. The moisture effect on the fatigue crack growth of glass particle and fiber reinforced epoxies with strong and weak bonding conditions Part 2. A microscopic study on toughening mechanism. Comp Sci Tech 2004;64(13–14):1991–2007.
[6] Nagasawa M, Kinuhata H, Koizuka H, Miyamoto K, Tanaka T, Kishimoto H, Koike T. Mechanical fatigue of epoxy resin. J Mater Sci 1995;30(5):1266–1272.
[7] Karger-Kocsis J, Friedrich K. Microstructure-related fracture toughness and fatigue crack growth behavior in toughened, anhydride-cured epoxy resins. Comp Sci Tech 1993;48(1–4):263–272.
[8] Becu L, Maazouz A, Sautereau H, Gerard JF. Fracture behavior of epoxy polymers modified with core-shell rubber particles. J Appl Polym Sci 1997;65(12):2419–2431.
[9] Rey L, Poisson N, Maazouz A, Sautereau H. Enhancement of crack propagation resistance in epoxy resins by introducing poly(dimethylsiloxane) particles. J Mater Sci 1999;34(8):1775–1781.
[10] Hayes BS, Seferis JC. Modification of thermosetting resins and composites through preformed polymer particles: a review. Polym Compos 2001;22(4):451–467.
[11] Azimi HR, Pearson RA, Hertzberg RW. Role of crack-tip shielding mechanisms in fatigue of hybrid epoxy composites containing rubber and solid glass spheres. J Appl Polym Sci 1995;58(2):449–463.
[12] Sautereau H, Maazouz A, Gerard JF, Trotignon JP. Fatigue behavior of glass bead filled epoxy. J Mater Sci 1995;30(7):1715–1718.
[13] McMurray MK, Amagi S. The effect of time and temperature on flexural creep and fatigue strength of a silica particle filled epoxy. J Mater Sci 1999;34(23):5927–5936.
[14] Brown EN, White SR, Sottos NR. Fatigue crack propagation in microcapsule toughened epoxy. J Mater Sci 2004;submitted.
[15] Azimi HR, Pearson RA, Hertzberg RW. Fatigue of hybrid epoxy composites: epoxies containing rubber and hollow glass spheres. Polym Engng Sci 1996;36(18):2352–2365.
[16] Paris PC, Gomez MP, Anderson WE. A rational analytic theory of fatigue. The Trend in Engineering, University of Washington 1961;13(1):9–14.
[17] Brown EN, White SR, Sottos NR. Microcapsule induced toughening in a self-healing polymer composite. J Mater Sci 2004;39(5):1703–1710.
[18] Elber W. Fatigue crack closure under cyclic tension. Engng Fract Mech 1970;2(1):37–45.
[19] Elber W. The significance of crack closure. Damage Tolerance in Aircraft Structures 1971; ASTM STP 486:230–242. American Society for Testing Materials.
[20] Ur-Rehman A, Thomason PF. The effect of artificial fatigue-crack closure on fatigue-crack growth. Fatig Fract Engng Mater Struct 1993;16(10):1081–1090.

[21] Song PS, Hwang S, Shin CS. Effect of artificial closure materials on crack growth retardation. Engng Fract Mech 1998;60(1):47–58.
[22] Sharp PK, Clayton JQ, Clark G. Retardation and repair of fatigue cracks by adhesive infiltration. Fatig Fract Engng Mater Struct 1997;20(4):605–614.
[23] Shin CS, Huang KC, Li RZ. Artificial retardation of fatigue crack growth by the infiltration of cracks by foreign materials. Fatig Fract Engng Mater Struct 1998;21(7):835–846.
[24] Galvin GD, Naylor H. Effect of lubricants on the fatigue of steel and other metals. Proceedings of the 1964 Institution of Mechanical Engineers 1965;170(3J):56–70.
[25] Endo K, Okada T, Komai K, Kiyota M. Fatigue crack propagation of steel in oil. Bull Jpn Soc Mech Engs 1972;15(89):1316–1323.
[26] Polk C, Murphy W, Rowe C. Determining fatigue crack propagation rates in lubricating environments through the application of a fracture mechanics technique. American Society of Lubrication Engineers (ASLE) Trans 1975;18(4):290–298.
[27] Plumbridge WJ. Mechano-environmental effects in fatigue. Mater Sci Engng 1977;27(3):197–208.
[28] Plumbridge WJ, Ross PJ, Parry JSC. Fatigue crack growth in liquids under pressure. Mater Sci Engng 1985;68(2):219–232.
[29] Tzou JL, Suresh S, Ritchie RO. Fatigue crack propagation in oil environments: 1. crack growth behavior in silicone and paraffin oils. Acta Metall 1985;33(1):105–116.
[30] Tzou JL, Hsueh CH, Evans AG, Ritchie RO. Fatigue crack propagation in oil environments: 2. A model for crack closure induced by viscous fluids. Acta Metall 1985;33(1);117–127.
[31] Davis FH, Ellison EG. Hydrodynamic pressure effects of viscous fluid flow in a fatigue crack. Fatig Fract Engng Mater Struct 1989;12(6):527–542.
[32] White SR, Sottos NR, Geubelle PH, Moore JS, Kessler MR, Sriram SR, Brown EN, Viswanathan S. Autonomic healing of polymer composites. Nature 2001;409(6822):794–797.
[33] Brown EN, White SR, Sottos NR. Retardation and repair of fatigue cracks in amicrocapsule toughened epoxy composite—Part II: *In situ* self-healing. Comp Sci Tech 2004; in review.
[34] Brown EN, Kessler MR, Sottos NR, White SR. In situ poly(urea-formaldehyde) microencapsulation of dicyclopentadiene. J Microencap 2003;20(16):719–730.
[35] Brown EN, Sottos NR, White SR. Fracture testing of a self-healing polymer composite. Exp Mech 2002;42(4):372–379.
[36] Mostovoy S, Crosley PB, Ripling EJ. Use of crack-line loaded specimens for measuring plane-strain fracture toughness. J Mater 1967;2(3):661–681.
[37] Simon SL, McKenna GB, Sindt O. Modeling the evolution of the dynamic mechanical properties of a commercial epoxy during cure after gelation. J Appl Polym Sci 2000;76(4):495–508.
[38] Yi KS, Cox BN, Dauskardt RH. Fatigue crack-growth behavior of materials in viscous fluid environment. J Mech Phys Solid 1999;47(9):1843–1871.

List of Recent TAM Reports

No.	Authors	Title	Date
978	Sofronis, P., I. M. Robertson, Y. Liang, D. F. Teter, and N. Aravas	Recent advances in the study of hydrogen embrittlement at the University of Illinois—Invited paper, Hydrogen–Corrosion Deformation Interactions (Sept. 16–21, 2001, Jackson Lake Lodge, Wyo.)	Sept. 2001
979	Fried, E., M. E. Gurtin, and K. Hutter	A void-based description of compaction and segregation in flowing granular materials—*Continuum Mechanics and Thermodynamics*, in press (2003)	Sept. 2001
980	Adrian, R. J., S. Balachandar, and Z.-C. Liu	Spanwise growth of vortex structure in wall turbulence—*Korean Society of Mechanical Engineers International Journal* **15**, 1741–1749 (2001)	Sept. 2001
981	Adrian, R. J.	Information and the study of turbulence and complex flow—*Japanese Society of Mechanical Engineers Journal B*, in press (2002)	Oct. 2001
982	Adrian, R. J., and Z.-C. Liu	Observation of vortex packets in direct numerical simulation of fully turbulent channel flow—*Journal of Visualization*, in press (2002)	Oct. 2001
983	Fried, E., and R. E. Todres	Disclinated states in nematic elastomers—*Journal of the Mechanics and Physics of Solids* **50**, 2691–2716 (2002)	Oct. 2001
984	Stewart, D. S.	Towards the miniaturization of explosive technology—Proceedings of the 23rd International Conference on Shock Waves (2001)	Oct. 2001
985	Kasimov, A. R., and Stewart, D. S.	Spinning instability of gaseous detonations—*Journal of Fluid Mechanics* (submitted)	Oct. 2001
986	Brown, E. N., N. R. Sottos, and S. R. White	Fracture testing of a self-healing polymer composite—*Experimental Mechanics* (submitted)	Nov. 2001
987	Phillips, W. R. C.	Langmuir circulations—*Surface Waves* (J. C. R. Hunt and S. Sajjadi, eds.), in press (2002)	Nov. 2001
988	Gioia, G., and F. A. Bombardelli	Scaling and similarity in rough channel flows—*Physical Review Letters* **88**, 014501 (2002)	Nov. 2001
989	Riahi, D. N.	On stationary and oscillatory modes of flow instabilities in a rotating porous layer during alloy solidification—*Journal of Porous Media* **6**, 1–11 (2003)	Nov. 2001
990	Okhuysen, B. S., and D. N. Riahi	Effect of Coriolis force on instabilities of liquid and mushy regions during alloy solidification—*Physics of Fluids* (submitted)	Dec. 2001
991	Christensen, K. T., and R. J. Adrian	Measurement of instantaneous Eulerian acceleration fields by particle-image accelerometry: Method and accuracy—*Experimental Fluids* (submitted)	Dec. 2001
992	Liu, M., and K. J. Hsia	Interfacial cracks between piezoelectric and elastic materials under in-plane electric loading—*Journal of the Mechanics and Physics of Solids* **51**, 921–944 (2003)	Dec. 2001
993	Panat, R. P., S. Zhang, and K. J. Hsia	Bond coat surface rumpling in thermal barrier coatings—*Acta Materialia* **51**, 239–249 (2003)	Jan. 2002
994	Aref, H.	A transformation of the point vortex equations—*Physics of Fluids* **14**, 2395–2401 (2002)	Jan. 2002
995	Saif, M. T. A, S. Zhang, A. Haque, and K. J. Hsia	Effect of native Al_2O_3 on the elastic response of nanoscale aluminum films—*Acta Materialia* **50**, 2779–2786 (2002)	Jan. 2002
996	Fried, E., and M. E. Gurtin	A nonequilibrium theory of epitaxial growth that accounts for surface stress and surface diffusion—*Journal of the Mechanics and Physics of Solids* **51**, 487–517 (2003)	Jan. 2002
997	Aref, H.	The development of chaotic advection—*Physics of Fluids* **14**, 1315–1325 (2002); see also *Virtual Journal of Nanoscale Science and Technology*, 11 March 2002	Jan. 2002
998	Christensen, K. T., and R. J. Adrian	The velocity and acceleration signatures of small-scale vortices in turbulent channel flow—*Journal of Turbulence*, in press (2002)	Jan. 2002
999	Riahi, D. N.	Flow instabilities in a horizontal dendrite layer rotating about an inclined axis—*Journal of Porous Media*, in press (2003)	Feb. 2002

List of Recent TAM Reports (cont'd)

No.	*Authors*	*Title*	*Date*
1000	Kessler, M. R., and S. R. White	Cure kinetics of ring-opening metathesis polymerization of dicyclopentadiene—*Journal of Polymer Science A* **40**, 2373–2383 (2002)	Feb. 2002
1001	Dolbow, J. E., E. Fried, and A. Q. Shen	Point defects in nematic gels: The case for hedgehogs—*Archive for Rational Mechanics and Analysis*, in press (2004)	Feb. 2002
1002	Riahi, D. N.	Nonlinear steady convection in rotating mushy layers—*Journal of Fluid Mechanics* **485**, 279–306 (2003)	Mar. 2002
1003	Carlson, D. E., E. Fried, and S. Sellers	The totality of soft-states in a neo-classical nematic elastomer—*Journal of Elasticity* **69**, 169–180 (2003) with revised title	Mar. 2002
1004	Fried, E., and R. E. Todres	Normal-stress differences and the detection of disclinations in nematic elastomers—*Journal of Polymer Science B: Polymer Physics* **40**, 2098–2106 (2002)	June 2002
1005	Fried, E., and B. C. Roy	Gravity-induced segregation of cohesionless granular mixtures—*Lecture Notes in Mechanics*, in press (2002)	July 2002
1006	Tomkins, C. D., and R. J. Adrian	Spanwise structure and scale growth in turbulent boundary layers—*Journal of Fluid Mechanics* (submitted)	Aug. 2002
1007	Riahi, D. N.	On nonlinear convection in mushy layers: Part 2. Mixed oscillatory and stationary modes of convection—*Journal of Fluid Mechanics* **517**, 71–102 (2004)	Sept. 2002
1008	Aref, H., P. K. Newton, M. A. Stremler, T. Tokieda, and D. L. Vainchtein	Vortex crystals—*Advances in Applied Mathematics* **39**, in press (2002)	Oct. 2002
1009	Bagchi, P., and S. Balachandar	Effect of turbulence on the drag and lift of a particle—*Physics of Fluids*, in press (2003)	Oct. 2002
1010	Zhang, S., R. Panat, and K. J. Hsia	Influence of surface morphology on the adhesive strength of aluminum/epoxy interfaces—*Journal of Adhesion Science and Technology* **17**, 1685–1711 (2003)	Oct. 2002
1011	Carlson, D. E., E. Fried, and D. A. Tortorelli	On internal constraints in continuum mechanics—*Journal of Elasticity* **70**, 101–109 (2003)	Oct. 2002
1012	Boyland, P. L., M. A. Stremler, and H. Aref	Topological fluid mechanics of point vortex motions—*Physica D* **175**, 69–95 (2002)	Oct. 2002
1013	Bhattacharjee, P., and D. N. Riahi	Computational studies of the effect of rotation on convection during protein crystallization—*International Journal of Mathematical Sciences*, in press (2004)	Feb. 2003
1014	Brown, E. N., M. R. Kessler, N. R. Sottos, and S. R. White	*In situ* poly(urea-formaldehyde) microencapsulation of dicyclopentadiene—*Journal of Microencapsulation* (submitted)	Feb. 2003
1015	Brown, E. N., S. R. White, and N. R. Sottos	Microcapsule induced toughening in a self-healing polymer composite—*Journal of Materials Science* (submitted)	Feb. 2003
1016	Kuznetsov, I. R., and D. S. Stewart	Burning rate of energetic materials with thermal expansion—*Combustion and Flame* (submitted)	Mar. 2003
1017	Dolbow, J., E. Fried, and H. Ji	Chemically induced swelling of hydrogels—*Journal of the Mechanics and Physics of Solids*, in press (2003)	Mar. 2003
1018	Costello, G. A.	Mechanics of wire rope—Mordica Lecture, Interwire 2003, Wire Association International, Atlanta, Georgia, May 12, 2003	Mar. 2003
1019	Wang, J., N. R. Sottos, and R. L. Weaver	Thin film adhesion measurement by laser induced stress waves—*Journal of the Mechanics and Physics of Solids* (submitted)	Apr. 2003
1020	Bhattacharjee, P., and D. N. Riahi	Effect of rotation on surface tension driven flow during protein crystallization—*Microgravity Science and Technology* **14**, 36–44 (2003)	Apr. 2003
1021	Fried, E.	The configurational and standard force balances are not always statements of a single law—*Proceedings of the Royal Society* (submitted)	Apr. 2003

List of Recent TAM Reports (cont'd)

No.	*Authors*	*Title*	*Date*
1022	Panat, R. P., and K. J. Hsia	Experimental investigation of the bond coat rumpling instability under isothermal and cyclic thermal histories in thermal barrier systems—*Proceedings of the Royal Society of London A* **460**, 1957–1979 (2003)	May 2003
1023	Fried, E., and M. E. Gurtin	A unified treatment of evolving interfaces accounting for small deformations and atomic transport: grain-boundaries, phase transitions, epitaxy—*Advances in Applied Mechanics* **40**, 1–177 (2004)	May 2003
1024	Dong, F., D. N. Riahi, and A. T. Hsui	On similarity waves in compacting media—*Horizons in World Physics* **244**, 45–82 (2004)	May 2003
1025	Liu, M., and K. J. Hsia	Locking of electric field induced non-180° domain switching and phase transition in ferroelectric materials upon cyclic electric fatigue—*Applied Physics Letters* **83**, 3978–3980 (2003)	May 2003
1026	Liu, M., K. J. Hsia, and M. Sardela Jr.	In situ X-ray diffraction study of electric field induced domain switching and phase transition in PZT-5H—*Journal of the American Ceramics Society* (submitted)	May 2003
1027	Riahi, D. N.	On flow of binary alloys during crystal growth—*Recent Research Development in Crystal Growth*, in press (2003)	May 2003
1028	Riahi, D. N.	On fluid dynamics during crystallization—*Recent Research Development in Fluid Dynamics*, in press (2003)	July 2003
1029	Fried, E., V. Korchagin, and R. E. Todres	Biaxial disclinated states in nematic elastomers—*Journal of Chemical Physics* **119**, 13170–13179 (2003)	July 2003
1030	Sharp, K. V., and R. J. Adrian	Transition from laminar to turbulent flow in liquid filled microtubes—*Physics of Fluids* (submitted)	July 2003
1031	Yoon, H. S., D. F. Hill, S. Balachandar, R. J. Adrian, and M. Y. Ha	Reynolds number scaling of flow in a Rushton turbine stirred tank: Part I—Mean flow, circular jet and tip vortex scaling—*Chemical Engineering Science* (submitted)	Aug. 2003
1032	Raju, R., S. Balachandar, D. F. Hill, and R. J. Adrian	Reynolds number scaling of flow in a Rushton turbine stirred tank: Part II—Eigen-decomposition of fluctuation—*Chemical Engineering Science* (submitted)	Aug. 2003
1033	Hill, K. M., G. Gioia, and V. V. Tota	Structure and kinematics in dense free-surface granular flow—*Physical Review Letters*, in press (2003)	Aug. 2003
1034	Fried, E., and S. Sellers	Free-energy density functions for nematic elastomers—*Journal of the Mechanics and Physics of Solids* **52**, 1671–1689 (2004)	Sept. 2003
1035	Kasimov, A. R., and D. S. Stewart	On the dynamics of self-sustained one-dimensional detonations: A numerical study in the shock-attached frame—*Physics of Fluids* (submitted)	Nov. 2003
1036	Fried, E., and B. C. Roy	Disclinations in a homogeneously deformed nematic elastomer—*Nature Materials* (submitted)	Nov. 2003
1037	Fried, E., and M. E. Gurtin	The unifying nature of the configurational force balance—*Mechanics of Material Forces* (P. Steinmann and G. A. Maugin, eds.), in press (2003)	Dec. 2003
1038	Panat, R., K. J. Hsia, and J. W. Oldham	Rumpling instability in thermal barrier systems under isothermal conditions in vacuum—*Philosophical Magazine*, in press (2004)	Dec. 2003
1039	Cermelli, P., E. Fried, and M. E. Gurtin	Sharp-interface nematic–isotropic phase transitions without flow—*Archive for Rational Mechanics and Analysis* **174**, 151–178 (2004)	Dec. 2003
1040	Yoo, S., and D. S. Stewart	A hybrid level-set method in two and three dimensions for modeling detonation and combustion problems in complex geometries—*Combustion Theory and Modeling* (submitted)	Feb. 2004
1041	Dienberg, C. E., S. E. Ott-Monsivais, J. L. Ranchero, A. A. Rzeszutko, and C. L. Winter	Proceedings of the Fifth Annual Research Conference in Mechanics (April 2003), TAM Department, UIUC (E. N. Brown, ed.)	Feb. 2004

List of Recent TAM Reports (cont'd)

No.	*Authors*	*Title*	*Date*
1042	Kasimov, A. R., and D. S. Stewart	Asymptotic theory of ignition and failure of self-sustained detonations—*Journal of Fluid Mechanics* (submitted)	Feb. 2004
1043	Kasimov, A. R., and D. S. Stewart	Theory of direct initiation of gaseous detonations and comparison with experiment—*Proceedings of the Combustion Institute* (submitted)	Mar. 2004
1044	Panat, R., K. J. Hsia, and D. G. Cahill	Evolution of surface waviness in thin films via volume and surface diffusion—*Journal of Applied Physics* (submitted)	Mar. 2004
1045	Riahi, D. N.	Steady and oscillatory flow in a mushy layer—*Current Topics in Crystal Growth Research*, in press (2004)	Mar. 2004
1046	Riahi, D. N.	Modeling flows in protein crystal growth—*Current Topics in Crystal Growth Research*, in press (2004)	Mar. 2004
1047	Bagchi, P., and S. Balachandar	Response of the wake of an isolated particle to isotropic turbulent cross-flow—*Journal of Fluid Mechanics* (submitted)	Mar. 2004
1048	Brown, E. N., S. R. White, and N. R. Sottos	Fatigue crack propagation in microcapsule toughened epoxy—*Journal of Materials Science* (submitted)	Apr. 2004
1049	Zeng, L., S. Balachandar, and P. Fischer	Wall-induced forces on a rigid sphere at finite Reynolds number—*Journal of Fluid Mechanics* (submitted)	May 2004
1050	Dolbow, J., E. Fried, and H. Ji	A numerical strategy for investigating the kinetic response of stimulus-responsive hydrogels—*Journal of the Mechanics and Physics of Solids* (submitted)	June 2004
1051	Riahi, D. N.	Effect of permeability on steady flow in a dendrite layer—*Journal of Porous Media*, in press (2004)	July 2004
1052	Cermelli, P., E. Fried, and M. E. Gurtin	Transport relations for surface integrals arising in the formulation of balance laws for evolving fluid interfaces—*Journal of Fluid Mechanics* (submitted)	Sept. 2004
1053	Stewart, D. S., and A. R. Kasimov	Theory of detonation with an embedded sonic locus—*SIAM Journal on Applied Mathematics* (submitted)	Oct. 2004
1054	Stewart, D. S., K. C. Tang, S. Yoo, M. Q. Brewster, and I. R. Kuznetsov	Multi-scale modeling of solid rocket motors: Time integration methods from computational aerodynamics applied to stable quasi-steady motor burning—*Proceedings of the 43rd AIAA Aerospace Sciences Meeting and Exhibit* (January 2005), Paper AIAA-2005-0357 (2005)	Oct. 2004
1055	Ji, H., H. Mourad, E. Fried, and J. Dolbow	Kinetics of thermally induced swelling of hydrogels—*International Journal of Solids and Structures* (submitted)	Dec. 2004
1056	Fulton, J. M., S. Hussain, J. H. Lai, M. E. Ly, S. A. McGough, G. M. Miller, R. Oats, L. A. Shipton, P. K. Shreeman, D. S. Widrevitz, and E. A. Zimmermann	Final reports: Mechanics of complex materials, Summer 2004 (K. M. Hill and J. W. Phillips, eds.)	Dec. 2004
1057	Hill, K. M., G. Gioia, and D. R. Amaravadi	Radial segregation patterns in rotating granular mixtures: Waviness selection—*Physical Review Letters*, in press (2004)	Dec. 2004
1058	Riahi, D. N.	Nonlinear oscillatory convection in rotating mushy layers—*Journal of Fluid Mechanics* (submitted)	Dec. 2004
1059	Okhuysen, B. S., and D. N. Riahi	On buoyant convection in binary solidification—*Journal of Fluid Mechanics* (submitted)	Jan. 2005
1060	Brown, E. N., S. R. White, and N. R. Sottos	Retardation and repair of fatigue cracks in a microcapsule toughened epoxy composite—Part I: Manual infiltration—*Composites Science and Technology* (submitted)	Jan. 2005
1061	Brown, E. N., S. R. White, and N. R. Sottos	Retardation and repair of fatigue cracks in a microcapsule toughened epoxy composite—Part II: *In situ* self-healing—*Composites Science and Technology* (submitted)	Jan. 2005